Journal of Pharmaceutical and Biomedical Analysis 51 (2010) 358–372

Contents lists available at ScienceDirect

Journal of Pharmaceutical and Biomedical Analysis

journal homepage: www.elsevier.com/locate/jpba

Review

MALDI-TOF MS analysis of plant proanthocyanidins

María Monagas[a], Jesús Eduardo Quintanilla-López[b,c], Carmen Gómez-Cordovés[a], Begoña Bartolomé[a], Rosa Lebrón-Aguilar[c,*]

[a] Instituto de Fermentaciones Industriales (CSIC), Juan de la Cierva 3, 28006 Madrid, Spain
[b] Departamento de Ingeniería Química Industrial y del Medio Ambiente, ETSI Industriales (UPM), José Gutiérrez Abascal 2, 28006 Madrid, Spain
[c] Instituto de Química-Física "Rocasolano" (CSIC), Serrano 119, 28006 Madrid, Spain

ARTICLE INFO

Article history:
Received 28 January 2009
Received in revised form 25 March 2009
Accepted 30 March 2009
Available online 7 April 2009

Keywords:
Mass spectrometry
MALDI-TOF
Proanthocyanidins
Food plants
Non-plant foods

ABSTRACT

Proanthocyanidins or condensed tannins are among the most abundant polyphenols compounds in our diet and may play a key role in the prevention of cardiovascular and neurodegenerative diseases and cancer. These antioxidants are widely distributed in the plant kingdom both in food plants and in non-food plants. The biological activity of plant proanthocyanidins depends on their chemical structure and concentration. However, due to their structural diversity and complexity, the qualitative and quantitative analysis of proanthocyanidins is a difficult task. Mass spectrometry has enabled great advances in the characterization of plant proanthocyanidins. Among these techniques, MALDI-TOF MS has proved to be highly suited for the analysis of highly polydisperse and heterogeneous proanthocyanidins. The objective of the present paper was to assess the potential, limitations and future challenges of the analysis of plant proanthocyanidins by MALDI-TOF MS techniques. Firstly, the fundamental of this technique, including modes of operation, advantages and limitations, as well as quantitative and qualitative operations, have been summarized. Applications of MALDI-TOF analysis to plant proanthocyanidins reported in the last decade (1997–2008) have been extensively covered, including the sample preparation protocols and conditions used for proanthocyanidin analysis, as well as the main findings regarding the determination of the structural features of different plant proanthocyanidin types (procyanidins, propelargonidins, prodelphinidins, profisetinidins and prorobinetinidins). Finally, attempts in the assessment of the molecular weight distribution of proanthocyanidins by MALDI-TOF are described.

Contents

* Corresponding author. Tel.: +34 915619400x1029; fax: +34 91564243.
E-mail address: rlebron@iqfr.csic.es (R. Lebrón-Aguilar).

0731-7085/$ – see front matter © 2009 Elsevier B.V. All rights reserved.
doi:10.1016/j.jpba.2009.03.035

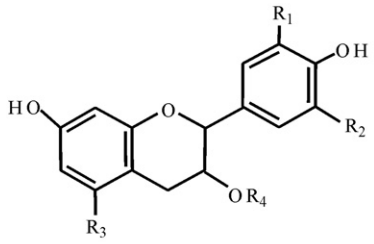

flavan -3-ol	R_1	R_2	R_3	R_4
(epi)afzelechin	H	H	OH	H
(epi)catechin	OH	H	OH	H
galloylated (epi)catechin	OH	H	OH	galloyl
(epi)gallocatechin	OH	OH	OH	H
(epi)fisetinidol	OH	H	H	H
(epi)robinetinidol	OH	OH	H	H

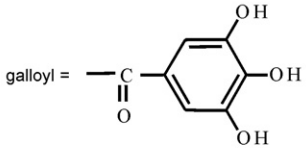

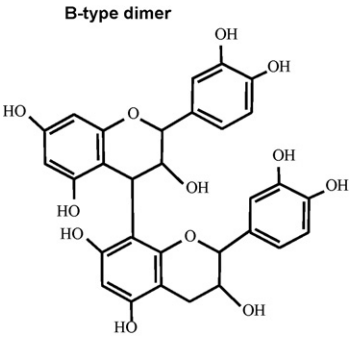

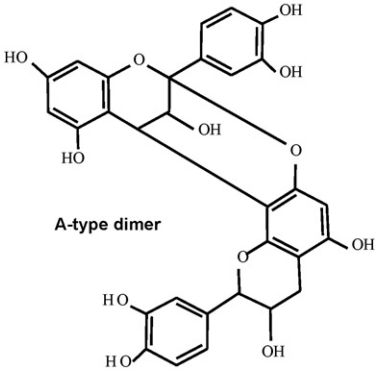

Fig. 1. Chemical structure of most common constitutive units of proanthocyanidins, and of B-type and A-type procyanidins.

1. Introduction

Proanthocyanidins or condensed tannins are polymers of flavan-3-ol that are widely distributed in the plant kingdom and are among the most abundant polyphenols in our diet. Besides their participation in food quality attributes such as astringency, bitterness, aroma and color formation, proanthocyanidin consumption has been associated with numerous health benefits due their antioxidant, anti-carcinogenic, cardioprotective, antimicrobial and neuro-protective activities [1]. Because of that they are considered as functional ingredients in botanical and nutritional supplements. However, the biological activity of plant proanthocyanidins depends on their chemical structure and concentration. Proanthocyanidin structure varies according to the [1,2]: (a) hydroxylation pattern of the A- and B-rings, (b) stereochemistry of C2, C3 and C4 of the central ring, and (c) interflavan linkages. The most common structural monomeric units of proanthocyanidins in plant foods are (+)-afzelechin, (+)-catechin and (+)-gallocatechin (2*R*:3*S* forms) and their diasteromers (-)-epiafzelechin, (-)-epicatechin and (-)-epigallocatechin (2*S*:3*S* forms), all of which possess a phloroglucinol type-A ring (Fig. 1). Some of these units could also be esterified with other molecules such as glucose or gallic acid (Fig. 1). Proanthocyanidins exclusively constituted by (epi)catechin are called procyanidins. Propelargonidins and prodelphinidins contain (epi)afzelechin and (epi)gallocatechin, respectively, and are usually mixed with procyanidins. Wood contains other constitutive units exhibiting a resorcinol type-A ring such as (epi)fisetinidin and (epi)robinetinidin which give rise to profisetinidins and prorobinetinidins, respectively. In relation to the interflavanic bond nature different regio- and stereoisomers can exist. B-type procyanidins are those in which monomers are linked through the C-4 position of the top unit and the C-6 or C-8 positions of the terminal unit, the C4–C8 isomers being more abundant than the C4–C6 ones, and frequently adopt the 3,4-*trans* stereochemistry. A-type procyanidins additionally contain an ether type bond between the C-2 position of the top unit and the hydroxyl group at C-5 or C-7 of the lower unit.

Due to the diversity and structural complexity of proanthocyanidins, the analysis and characterization of proanthocyanidins is a difficult task [3]. As the molecular weight increases over a degree of polymerization (DP) of 4, the possible number of regio- and stereoisomers becomes very large making reversed-phase HPLC separation very difficult. However, this technique can be applied for the recognition of the extension and terminal structural units of proanthocyanidins after acid-catalyzed depolymerization in the presence of nucleophilic reagents such as phloroglucinol [4] or toluene α-thiol [5], allowing the determination of the mean DP, among other parameters. Normal-phase HPLC has been applied to separate proanthocyanidins according to their molecular weight in various plant foods up to DP10 [6,7]. Nevertheless, separation becomes difficult when galloylated units are also present. Other techniques, such as mass spectrometry (MS) are more suitable for the estimation of the molecular mass distribution of heterogeneous proanthocyanidins in complex mixtures. The purpose of mass spectrometers is to detect gas-phase ions, either positive or negative, separated according to their mass-to-charge ratio (m/z). Historically, the two most common ionization techniques used to generate gaseous ions from an analyte are electron impact (EI) and chemi-

cal ionization (CI), which require vaporization before ionization. However, most biological, natural and synthetic materials are non-volatile, and often thermally labile, so the conventional ionization techniques are not suitable for MS analyses. To increase volatility, in some cases derivatization of the compounds may be performed, but interpretation of the fragmentation patterns becomes difficult. These facts limited the investigation of high molecular mass substances by MS in the past. A variety of new ionization methods, which enable simultaneous volatilization and ionization of the analyte molecules directly from the sample, were developed spreading the type and molecular mass range of compounds to be analyzed. However, it was not until 1988 with the development of electrospray ionization (ESI) [8] and matrix-assisted laser desorption/ionization (MALDI) [9,10] when MS extended the mass range beyond 300,000 u for proteins [11] and 1500,000 u for synthetic polymers [12] and had an enormous impact on the use of MS in biology and the life sciences. In the analysis of plants proanthocyanidins, ESI provides cationic or anionic species with little or no fragmentation and has been widely used to characterize this type of compounds in foods [13–17], however it is not well suited for the analysis of highly polydisperse proanthocyanidins due to the generation of multiply charged ions which makes difficult the interpretation of the spectra. For the analysis of complex proanthocyanidin samples without LC separation, MALDI offers several advantages over ESI including a greater tolerance for impurities, the detection of predominantly single-charged molecular ions, the possibility of reanalyze the same sample, and the optimal compatibility with simple and not very expensive time-of-flight (TOF) analyzers due to its pulsed nature. The almost unlimited mass range of TOF analyzers and its ability to acquire the entire spectrum from a single laser pulse event are other factors in favor of the MALDI-TOF combination.

The objective of this paper was to assess the potential, limitations and future challenges of the analysis of plant proanthocyanidins by MALDI-TOF MS. For that aim, we have reviewed the scientific literature concerning this topic over the last 10 years (1997–2008). Some unpublished data from our laboratory are also included in order to illustrate the spectra display obtained from the application of different operation modes. The paper has been divided in two main parts: I. MALDI-TOF MS technique, which summarizes the fundamentals, modes of operation, and advantages and limitations of the technique, as well as quantitative and qualitative operations, and II. Applications of MALDI-TOF analysis to plant proanthocyanidins, which reports the use of this technique to the characterization of proanthocyanidins from different substrates, including food and non-food plants. Since sample preparation is indeed a crucial step in MALDI-TOF analysis, the protocols and conditions used have been revised (Section 3.1). Main findings regarding the determination of the structural features of different plant proanthocyanidin types (procyanidins, propelargonidins, prodelphinidins, profisetinidins and prorobinetinidins) by MALDI-TOF MS are also reported (Section 3.2). Finally, attempts in the assessment of the molecular weight distribution of proanthocyanidins by MALDI-TOF MS are described (Section 3.3).

2. MALDI-TOF MS technique

2.1. Fundamentals of the MALDI process

Molecules naturally possess rotational, vibrational, electronic, and, in the case of gases and liquids, kinetic energy. If a molecule or group of molecules in a solid have their internal energy increased (e.g., by heat or radiation) over a relatively long period of time (a few microseconds), the molecules can equilibrate the energy individually and together so that the excess energy is dissipated to the surroundings without causing any change in molecular structure. However, putting much energy into a sample in a very short space of time (e.g., a laser pulse), the energy cannot be dissipated to its surroundings fast enough and the sample is simply blasted away from the target area because of a large gain in kinetic energy. This process can cause melting, vaporization, possible destruction of material and, important for MS, ionization of analytes [18]. This is the basis of laser desorption/ionization (LDI), which have been used since 1960 for the analysis of organic and inorganic salts, pigments, etc. Nevertheless, it is limited to masses below 1000 u, as the energy transfer is difficult to control and often leads to excessive thermal degradation. The main breakthrough toward higher masses was achieved by embedding the analyte molecules in low concentration into a solid or liquid highly light-absorbing matrix. In this way, an efficient and controllable energy transfer was realized by guarding the molecules from excessive amounts of energy. This technique became known as MALDI and has significantly revolutionized approaches to the study of large biological and synthetic polymers.

Although thousands of papers have been published on MALDI applications, the detailed mechanism of MALDI process, especially the ionization step itself, is far less understood. Two major models; namely photochemical ionization [19] and cluster ionization [20] mechanisms have been proposed to explain many of the experimental results. With the photochemical ionization model, analyte ions are considered to be produced from a protonation or deprotonation process involving an analyte molecule colliding with a matrix ion in the gas phase. According to the cluster ionization model, charged particles are desorbed with a strong photoabsorption by matrix molecules. Analyte ions are subsequently produced by desolvation of matrix from cluster ions. Nevertheless, many facts still cannot be explained by these two models, and new ones based on a pseudo proton transfer process during crystallization as a primary mechanism for producing analyte ions have been presented [21].

2.2. Experimental parameters

In general, a MALDI-TOF analysis is initiated by mixing the analytes solution (~10 μM) with a large molar excess (~50 mM) of the host matrix solution and depositing about one microliter of the mixture on a stainless steel sample target. After evaporating the solvent, the sample–matrix crystals are irradiated with a laser beam of high irradiance power (10^6 W cm^{-2}) and short pulse width (few nanoseconds) to simultaneously desorb and ionize the sample and matrix molecules into the gas. The packs of ions are accelerated by a fixed electrical potential into the analyzer (1–2 m flight path) and finally, they hit the detector. In this way, the m/z values for the analyte ions are calculated as a function of their *times of flight*, and thus, the mass spectrum is obtained. Several factors affect the appearance of a MALDI-TOF spectrum and therefore, the information provided. Sensitivity, selectivity and mass resolution among other performance parameters are strongly influenced on the following factors:

2.2.1. Matrix selection and sample preparation

An ideal matrix should have the following properties: (1) strong absorption of radiation at the laser wavelength; (2) good mixing and solvent compatibility with the analyte; (3) good vacuum stability and low vapor pressure; and (4) participation in some kind of photochemical reactions. Generally, the choice and discovery of new matrix materials have been achieved more or less empirically and appear not to be related to the analyte in terms of structure or physical properties.

Solid organic matrices are the most common type. However, a critical problem during sample preparation for MALDI-TOF analysis using these matrices is the possibility of segregation of the analyte

and matrix molecules during co-crystallization process, resulting in inhomogeneous sample preparations that create sample-to-sample and spot-to-spot variations in the analyte signal. Several sample preparation techniques are available (i.e. fast-evaporation, sandwich matrix, spin-dry, seed-layer technique, electrospray deposition and solvent-free sample preparation, among others), all with the aim of achieving fine-grained homogeneous crystal formation. However, no universal sample preparation for a broad type of analyte molecules exists. The most common procedure is the so-called dried droplet method. In this method, the sample solution is mixed with an equal volume of the saturated matrix solution (prepared in the same medium) in a molar ratio of 1000:1 to 10,000:1. A drop of that mixture is applied onto the MALDI target and is dried slowly in the ambient air or by a gentle stream of cold air. Drying the sample spot under vacuum or in a refrigerator can improve the homogeneity of the sample preparation. Organic liquids, ionic liquids and inorganic materials have also been used instead of traditional solid organic matrices to overcome this inhomogeneity [22].

Finally, it must be pointed out that, although MALDI is relatively tolerant to sample impurities, such as salts, buffer compounds or surfactants, the quality of mass spectra usually degrades when the salt concentration is higher than ca. 100 mM. Sample dilution, dialysis, cation exchange, solid phase extraction, liquid chromatography, as well as some recent clean-up methods that occur directly on the MALDI sample probe have been used [23].

2.2.2. Cationization agent

When the compounds to be analyzed are not easily protonated, they can be cationized, by adding an organic or inorganic salt, depending on their solubility, to the matrix/sample mixture. A right choice of the cationization agent improves the spectrum recording, increases the signal-to-noise ratio and suppresses signals caused by other salts present in the sample. Analytes with electronegative elements like oxygen or nitrogen are best cationized by Li^+ or Na^+, whereas analytes with π-electrons prefer large polarizable cations like Ag^+ or Cu^{2+}.

2.2.3. Laser

UV and IR laser systems have found applications in MALDI analysis, but the vast majority of commercial MALDI instruments use the UV nitrogen laser (337 nm). Both lasers yield similar spectra, although better resolution has been obtained for some proteins with an IR laser. Experimentally, certain energy threshold value has been found necessary for the generation of meaningful mass spectra. This threshold value is fairly sharp and has to be optimized since very high laser irradiance leads to an increase in the signal-to-noise ratio but a decrease in the mass resolution. As a general rule, a laser irradiance of about 20% above the threshold is used.

2.2.4. TOF analyzer

The principle of operation of TOF analyzers is quite simple: ions of different m/z are dispersed in time during their flight along a field-free drift path of known length. Provided all ions start their journey at the same time, the lighter ones will reach the detector earlier than the heavier ones. For optimal performance, this process demands a pulsed ionization method, as MALDI. The main advantages of TOF instruments are: (a) theoretically, unlimited mass range; (b) for each ionizing event, a complete mass spectrum is obtained within several tens of microseconds; (c) high sensitivity, due to their high ion transmission; (d) the construction of a TOF analyzer is comparatively straightforward and not very expensive; and (e) recent instruments allow for accurate mass measurements and tandem MS experiments [24].

Mass resolution is the ability of an instrument to separate the signals from ions of similar m/z. In the case of MALDI-TOF MS, because the ions have a certain time-span of formation, a spatial distribution, and a kinetic energy spread, the resolution is especially poor. The ions of the same m/z reach the detector in a wide distribution that increases as the molecular masses do. Therefore, the peak widths for high m/z ions are greater than those for low m/z ions. Consequently, the isotopic peaks of the ions are more difficult to resolve as the m/z increase.

Improvements in mass resolution can be obtained by instrument modification. For example, an ion mirror, or reflectron, compensates for the initial energy spread of the created ions by a retarding electrical field at the end of the flight tube. The ions penetrate the reflectron until they reach zero kinetic energy and then expelled in opposite direction. This process greatly increases the mass resolution, especially for analytes with molecular masses lower than 4000 u. When the molecular masses are higher than 10,000 u, no resolution improvement is observed because the reflectron process generates loss of small neutrals (NH_3, H_2O, CO_2) from the analyte causing an additional broadening of the peak profile [25]. Alternatively, peak broadening due to the time spread ion formation can be reduced by the application of "delayed extraction" [26], that involves forming the ions in a field-free region and applying a high-voltage pulse to accelerate the ions. The extraction pulse is delayed with respect to firing the laser by a few hundred nanoseconds. Thus, the initial desorption and ion formation processes are separated from the ion acceleration step and, therefore, the time window required for ion formation does not contribute to peak broadening.

2.3. Qualitative and quantitative analysis

MALDI-TOF mass spectra of pure compounds are normally dominated by a single ion corresponding to the protonated molecule; multiply charged ions are rare, except for very large molecules and even then, they are usually of low relative abundance. Spectra of mixtures typically show multiple ions corresponding to the protonated forms of some if not all of the molecular components present in the sample. In addition, the adducts of the molecule with Na^+ and K^+ are also a common feature of the MALDI-TOF spectra of biological samples or when the analyte does not show acidic characteristics. Negative-ion analysis can also be performed with MALDI-TOF MS, but only used for specific analytes (e.g., nucleotides) because of the low sensitivity. The spectrum region below about m/z 500 is not very informative because it is saturated with signals from matrix-derived ions, so most of the times is not shown.

Prerequisite of spectra interpretation is the mass calibration of the MALDI-TOF spectrometer in order to make use of one of their advantages, the absolute mass scale. The external mass calibration procedure is usually adopted. It consists in recording the spectrum of one or two compounds of known mass and computing a set of calibrating constants that will be then applied in the analysis of unknown compounds.

Ions can be detected in the linear and reflectron modes, which are complementary since high resolution is obtained in the reflectron mode, whereas high sensitivity, especially at high molar mass, is achieved in the linear mode. Both detection methods have advantages and drawbacks and ought to be chosen according to the information desired. Generally, the linear mode is used to analyze proteins, complex mixtures or polymeric distributions, especially when they have high molecular masses (more than 10,000 u), whereas the reflection mode is used preferentially for determining the accurate molar mass of individual species below 10,000 u.

From a quantitative point of view, it is noteworthy that peak heights for equimolar loadings of different analytes may vary significantly and are not usually representative of its abundance in solution. Moreover, there is substantial variability in the noise level, baseline and peak intensities in a collection of MALDI-TOF spectra generated from the same sample. Variations in ion current are observed with consecutive laser shots fired at the same posi-

tion on the target, across different locations on the target surface and between identical loadings of the same sample onto different targets. To minimize this variability, multiple spectra are usually acquired from different locations across the target surface and these are averaged to yield a more representative spectrum. The primary contributor to this variability is heterogeneous incorporation of the analyte into the co-crystallized matrix–analyte complex. Competitive ionization/ion suppression is an additional factor that can obliterate any attempt to quantify by MALDI, especially in complex samples. Consequently, when quantifying across a series of samples it is essential to keep the sample composition constant [27].

Therefore, although quantitative analyses by MALDI-TOF MS have been reported [28,29], a careful optimization of the experimental parameters and sample preparation (i.e., matrix, concentration, solvents, crystallization conditions), the use of internal standards for calibration and the averaging of multiple spectra are required in order to reduce the great variability observed [30].

3. Applications of MALDI-TOF MS analysis to plant proanthocyanidins

3.1. Extraction and preparation of plant materials for MALDI-TOF MS

Table 1 presents the conditions reported in the literature for the extraction of proanthocyanidins from plant materials, and further purification and fractionation steps. The sample concentration, matrixes, and cationization agents used for the sample preparation for MALDI-TOF analysis are also given. Data in Table 1 are chronologically organized to better show the evolution of these conditions over time.

With the exception of the novel approach carried out by Ishida et al. [31], in which the pulverized sample was directly analyzed without previous extraction, the extraction of proanthocyanidins from plant materials for MALDI-TOF analysis is usually carried out by liquid extraction using pure acetone and methanol, as well as acetone/water (50:50, 70:30–90:10, v/v), or ethanol or methanol/water (or acidified water) (50:50–80:20, v/v) mixtures, followed or not by subsequent ethyl acetate extraction (Table 1). Some authors have employed solvent extraction on solid supports such as Sepabeads SP-850 [32,33] and Sephadex LH20 [34] columns. Hexane, chloroform, dichloromethane, trichloromethane and petroleum ether are frequently used before or after the previous liquid extraction for eliminating lipids and pigments from fatty substrates. The resulting extracts could be further purified on TSK gel Toyopearl HW-40EC, Toyopearl HW-40S, Sephadex LH20 or LiChrospher 100 (Table 1). Subsequent fractionation of proanthocyanidin from the purified extract could also be carried out in some of the above mentioned media or in other supports such as Relite SP411 and Diaion HP-20ss. The purified or isolated proanthocyanidin sample could be then lyophilized. Isolation of proanthocyanidins could also be performed by gravimetric methods such as ytterbium acetate precipitation [35]. Other treatments such as acetylation with pyridine-acetic anhydride have also been employed for the stabilization of the proanthocyanidin compounds [36,37]. Finally, for MALDI-TOF analysis, lyophilized samples are resuspended in pure methanol, acetone, acetonitrile, tetrahydrofuran or in acetone/water (80:20, v/v) and acetonitrile/water (50:50, v/v) mixtures in a concentration ranging from 0.5 to 18 mg/mL (Table 1). In summary, due their large structural complexity, isolation of proanthocyanidins from the plant material is an intensive labour and could be accomplished by a wide range of techniques. Among these techniques, adsorption chromatography on Sephadex and Toyopearl has proved to be very suitable for sample clean up and fractionation of proanthocyanidins according to their molecular weight. As it will be discussed in Section 3.3, purification and fractionation of proanthocyanidins have been demonstrated to be a crucial step in enhancing sensitivity under MALDI-TOF MS.

Although commonly used matrices for MALDI-TOF analysis, such as α-cyano-4-hydroxycinnamic acid, sinapinic acid, 9-nitroanthracene, 5-chlorosalicylic acid, 2-(4-hydroxyphenylazo)-benzoic acid and dithranol have been tested [32,38], only 2,5-dihydroxybenzoic acid (DHB) and *trans*-3-indoleacrylic acid (*t*-IAA) have been demonstrated to be highly suited for the detection of proanthocyanidins by MALDI-TOF MS. According to Ohnishi-Kameyana et al. [32], *t*-IAA was efficient for the detection of dimers and condensed tannins but not for the detection of monomers, whereas DHB was suited for the detection monomers and condensed tannins but failed to detected dimeric forms. In contrast, experiments performed by Yang and Chien [38] revealed that DHB was successful for the detection of the three types of forms since it provided the widest mass range and the least background noise. *t*-IAA and DHB are normally employed in a concentration ranging from 10 to 100 mg/mL or up to saturation, in solvent such as water, methanol, acetonitrile, tetrahydrofuran, or methanol/water (40:60, v/v), acetone/water (70:30 and 80:20, v/v), and acetonitrile/water (2:3, v/v) mixtures. The sample and matrix are usually combined in a 1:1 (v/v) sample-to-matrix ratio and then deposited on the target plate. In some studies, a cationization agent such as sodium chloride [37,39,40] or sodium iodide [31,36,41] has been employed to increase the detection of $[M+Na]^+$ adducts. Silver trifluoroacetate has proved to be successful in improving the sensitivity of the detection of apple procyanidins as $[M+Ag]^+$ adducts [32]. For substrates presenting proanthocyanidins with a high degree of heterogeneity, cesium trifluoroacetate was used to eliminate naturally occurring $[M+K]^+$ adducts that could lead to a misinterpretation of mass spectra signals [42,43]. The ratio of sample:matrix:cationization agent employed is usually 1:10:1 (v/v/v) (Table 1).

3.2. Determination of proanthocyanidin structure by MALDI-TOF MS

A summary of the application of MALDI-TOF MS to the characterization of different types of proanthocyanidins in plant and non-plant foods, showing the operation mode, mass species, DP range, observed masses, structural constitutive units and other structural features (galloyl groups and A-type bonds), is presented in Tables 2 and 3.

In MALDI-TOF MS, the positive mode has been demonstrated to be more suited for this type of compounds (Tables 2 and 3). Mass data for proanthocyanidins has been usually reported as naturally occurring $[M+Na]^+$ and $[M+K]^+$ adducts, but $[M+Ag]^+$ and $[M+Cs]^+$ adducts have also been reported in some cases depending on the cationization agent employed (Table 1). Assignation of MALDI-TOF mass signals to a particular proanthocyanidin structure can be achieved by the determination of the theoretical or calculated mass. The theoretical monoisotopic mass (as sodium adducts, $[M+Na]^+$) corresponding to the different classes of proanthocyanidins (procyanidins, propelargonidins, prodelphinidins, profisetinidins and prorobinetinidins) can be calculated as:

$$[M+Na]^+ = 290.08 * CAT + 274.08 * AFZ + 306.07 * GCAT + 274.08 * FIS + 290.08 * ROB + 152.01 * GALLOYL - 2.02 * B - 4.04 * A + 22.99$$

where *CAT*, *AFZ*, *GCAT*, *FIS* and *ROB* are, respectively, the numbers of (epi)catechin, (epi)afzelechin, (epi)gallocatechin, (epi)fisetinidol and (epi)robinetinidol units contained in the proanthocyanidin molecule, *GALLOYL* are the numbers of galloyl ester units attached to the flavan-3-ol units, and *B* and *A* are, respectively, the numbers

Table 1
Data reported on the extraction and preparation of plant proanthocyanidins for MALDI-TOF MS analysis.

Reference	Substrate	Extraction	Further treatment	Sample concentration, solvent	Matrix: concentration, solvent	Cationization agent: concentration, solvent	Sample/matrix/ cation ratio
Ohnishi-Kameyama et al. [32]	Apple juice	EtOH (80:20, v/v) on Sepabeads SP-850 column	Purification and fractionation on TSKgel toyopearl HW-40EC column	0.5 mg/mL, acetone	*t*-IAA: 10 mg/mL	Silver trifluoroacetate: 1mM, acetone	2:1:1 (v/v)
Yang and Chien [38]	Grape seeds	Acetone/water (50/50, w/w) Ethyl acetate		2 mg/mL, acetone or MeOH	DHB: 20 mg/mL, THF *t*-IAA		1:1 (v/v)
Foo et al. [16]	Cranberries	Acetone Petroleum ether Ethyl acetate	Purification on Sephadex LH20 column				
Hedqvist et al. [56]	*Lotus corniculatus* (var. Fargus)	Acetone/water (70:30, v/v)	Purification and fractionation on Sephadex LH-20 column	18 mg/mL, acetone/water (80:20, v/v)	*t*-IAA		100 μL sample/5 mg matrix
Krueger et al. [35]	Grape seeds	Acetone/water (70:30, v/v)	Ytterbium acetate and triethanolamine precipitation	18 mg/mL, acetone/water (80:20, v/v)	*t*-IAA		100 μL sample/5 mg matrix
Pasch et al. [57]	-Quebracho (*Schinopsis balansae)* tannin extract -Mimosa bark (*Acacia mearnsii)* tannin extract	Dissolution in acetone		10 mg/mL	DHB: 10 mg/mL, acetone	NaCl	1:1 (v/v)
Porter et al. [52]	Cranberries (concentrate juice powder)		Purification and fractionation on Sephadex LH20 column		t-IAA: 100 mg/mL		1:1 (v/v)
Takahata et al. [48]	Brown soybean seed coat	Acetone/water (70:30, v/v)	Fractionation on Sephadex LH-20 column	0.5 mg/mL, acetone	*t*-IAA: 10 mg/mL		1:1 (v/v)
Behrens et al. [54]	-Willow leaves (*Salix alba*) -Lime leaves (*Tilia cordata*) -Beach leaves (*Fagus sylvatica*) -Spruce needles (*Picea abies*)	Hexane Acetone/water (70:30, v/v) Ethyl acetate Chloroform	Purification on Sephadex LH-20 column	Acetonitrile/water (50:50, v/v)	DHB: acetonitrile/water (50:50, v/v)		
Krueger et al. [42]	Sorghum (*Sorghum bicolor (L.) Moench)*	Acetone/water (70:30, v/v)	Fractionation on Sephadex LH-20 column		*t*-IAA: 50 mg/mL, acetone/water (80:20, v/v)	Cesium trifluoroacetate	1:1 and 1:2 (v/v)
Perret et al. [51]	Grape berries	MeOH/acetone/water (40:40:20, v/v/v) Hexane	Purification on LH-20 column and Toyopearl HW-40S Fractionation on Relite SP411 column	10 mg/mL, MeOH	DHB:saturated, MeOH/water (40:60, v/v)		0.3 μL/1 μL (1:2.3, v/v)
Taylor et al. [17]	Hops (*Humulus Lupulus L.*)	Dichloromethane Acetone/water (70:30, v/v) Dichloromethane and Hexane	Purification and fractionation on Sephadex LH-20 column	1–2 mg/mL, AcN	t-IAA, saturated, AcN		
Nonier et al. [36]	Grape seeds	EtOH/acidified water (acetic acid, 10%) (1:1, v/v) Chloroform	Acetylation with pyridine-acetic anhydride (1:1, v/v)	10 mg/mL, THF	DHB: 10 mg/mL, THF	NaI: 10 mg/mL, MeOH	1:10:1 (v/v/v)
Ramírez-Coronel et al. [46]	Coffe pulp (*Coffea arabica*)	Hexane MeOH (2.5% acetic acid) Acetone/water (2:3) (2.5% acetic acid)		0.5 mg/mL, MeOH	DHB: 10 mg/mL, MeOH		1:1 (v/v)
Rösch et al. [34]	Sea buckthorn (*Hippophae rhamnoides*) pomace	Extraction on Sephadex LH-20 column	Fractionation on Sephadex LH-20 column	10 mg/mL	DHB: 10 mg/mL, AcN/water (with TFA 0.1%) (2:3, v/v)		
Vivas et al. [41]	Heartwood of Quebracho (*Schinopsis balansae*)	Acetone/water (70:30, v/v)		10 mg/mL, MeOH	DHB: 10 mg/mL, MeOH	NaI: 10 mg/mL, MeOH	1:10:1 (v/v/v)
Vivas et al. [41]	Grape seeds, skins and stems	EtOH/acidified water (50:50, v/v) Chloroform		10 mg/mL, MeOH	DHB: 10 mg/mL, MeOH	NaI: 10 mg/mL, MeOH	1:10:1 (v/v/v)
Ishida et al. [31]	Bark of *Acacia auriculiformis*	No extraction; direct analysis of the solid sample		1 mg	DHB: 125 mM, MeOH + 1% (v/v) TFA	NaI: 1 mM, MeOH	5mg/500 μL (DHB + TFA solutions)

Table 1 (*Continued*)

Reference	Substrate	Extraction	Further treatment	Sample concentration, solvent	Matrix: concentration, solvent	Cationization agent: concentration, solvent	Sample/matrix/cation ratio
Es-Safi et al. [49]	Pear juice	Dilution with acidified water	Purification on LiChrospher 100 RP-18 column	0.018 mg/mL, AcN/water (50:50, v/v)	DHB		1:1 (v/v)
Meagher et al. [55]	Flower of *Trifolium spp.*	Acetone/water (70:30, v/v) Dicloromethane	Purification on Sephadex LH-20 column	0.5 mg/mL, acetone/water (80:20, v/v)	DHB: 10 mg/mL, acetone/water (80:20, v/v)	NaCl: 0.1M	1:1 (v/v)
Neto et al. [43]	Cranberries	Acetone/methanol/water/formic acid (40:40:19:1, v/v)	Purification on C18 and Sephadex LH-20 Fractionation on Toyopearl HW-40C	15 mg/mL, acetone/water (80:20, v/v)	*t*-IAA: 50 mg/mL, acetone/water (80:20, v/v)	Cesium trifluoroacetate	1:2 (v/v)
Shoji et al. [33]	Apple juice	EtOH (80:20, v/v) on Sepabeads SP-850 colum	Fractionation on Diaion HP-20ss column	0.5 mg/mL, MeOH	THAP: 10 mg/mL, acetone		1:1 (v/v)
Sivakumaran et al. [39]	*Lotus spp.*	Acetone/water (70:30, v/v) Dichloromethane	Purification and fractionation on Sephadex LH-20 column	0.5 mg/mL, acetone/water (80:20, v/v)	DHB: 10 mg/mL, acetone/water (80:20, v/v)	NaCl: 0.1 M	1:1 (v/v)
Ku and Mun [37]	Bark of *Pinus radiata*	Water 100 °C Acetone/water (70:30, v/v) Hexane Ethyl acetate	Purification on Sephadex LH-20 column Acetylation with pyridine-acetic anhydride (1:1, v/v)		DHB: acetone/water (70:30, v/v)	NaCl, acetone (70:30, v/v)	1:10:1 (v/v/v)
Monagas et al. [53]	Almond (*Prunus dulcis (Mill.) D.A. Webb*) skins	MeOH/HCl (1000:1, v/v) Ethyl acetate			DHB: 20 mg/mL, water		1:4 (v/v)
Spencer et al. [40]	Dock (*Rumex obtusifolius*)	Acetone/water (70:30, v/v) Dichloromethane	Purfication and fractionation on Sephadex LH-20 column	0.5 mg/mL, acetone/water (80:20, v/v)	DHB: 10 mg/mL, acetone/water (80:20, v/v)	NaCl: 0.1 M	1:1 (v/v)
Strek et al. [47]	Japanese quince fruit (*Chaenomeles japonica*)	Acetone/water (90:10, v/v) Trichlomethane Ethyl acetate			DHB		
Weber et al. [50]	*Pinus pinaster* bark extract *Pinus massoniana* bark extract Grape seed extract			5–10 mg/mL, MeOH	DHB: 20 mg/mL, MeOH		1:1 (v/v)

t-IAA: trans-3-indoleacrylic acid; DHB: 2,5-dihydroxybenzoic acid; THF: tetrahydrofuran; TFA: trifluoracetic acid; THAP: trihydroxyacetophenone.

Table 2
Structural characterization of proanthocyanidins from food plants by MALDI-TOF MS analysis.

Substrate	Mode[a]	Mass specie	DP range	Observed mass	CAT	FIS	AFZ	GCAT	ROB	Galloyl	A-type bond	Proanthocyanidin type	Reference
Apple juice	Linear	$[M+Ag]^+$	3–15	nr	DP							B-type procyanidins	Ohnishi-Kameyama et al. [32]
Apple juice	Linear	$[M+Na]^+$	6–10	1754–2907	DP							B-type procyanidins	Shoji et al. [33]
		$[M+K]^+$	6–10	1770–2923	DP								
Apples	Reflectron	$[M+Na]^+$	2–15	nr	DP							B-type procyanidins	Mané et al. [45]
		$[M+K]^+$	4–13	nr	DP								
Brown soybean seed coat	Linear and reflectron	$[M+K]^+$	5–30	nr	DP							B-type procyanidins	Takahata et al. [48]
Coffe pulp (*Coffea arabica*)	Linear	$[M+Na]^+$	2–6	600–1753	DP							B-type procyanidins	Ramírez-Coronel et al. [46]
Japanese quince fruit (*Chaenomeles japonica*)	Reflectron	$[M+Na]^+$	2–9	602–2626	DP							B-type procyanidins	Strek et al. [47]
		$[M+K]^+$	1–3, 5–6	332–906, 1483–1772	DP								
Pear juice	Linear and reflectron	$[M+Na]^+$	4–24	nr	DP					0		B-type procyanidins, galloylated	Es-Safi et al. [49]
			3–23	nr	DP					1			
Grape seeds	Reflectron	$[M+Na]^+$	1–6	313.13–1753.68	DP					0		B-type procyanidins, galloylated	Yang and Chien [38]
			1–7	465.17–2193.76	DP					1			
			2–7	905.33–2346.80	DP					2			
	Linear	$[M+Na]^+$	8, 9	2633, 2921	DP					2			
			7, 8, 9	2497, 2785, 3073	DP					3			
			7, 8	2649, 2937	DP					4			
			6, 7, 8	2513, 2801, 3089	DP					5			
			6, 8	2665, 3241	DP					6			
Grape seeds	Reflectron	$[M+Na]^+$	2–9	601–2618	DP					0		B-type procyanidins, galloylated	Krueger et al. [35]
			2–8	753–2483	DP					1			
			2–7	905–2346	DP					2			
			3–5, 7	1345–1922, 2499	DP					3			
			4–6	1786–2362	DP					4			
	Linear	$[M+Na]^+$	2–11	600–3194	DP					0			
			2–11	752–3349	DP					1			
			2–10	905–3212	DP					2			
			3–9	1346–3075	DP					3			
			4–8	1785–2938	DP					4			
			6–8	2513–3090	DP					5			
			6–7	2667–2954	DP					6			
Grape seeds	Reflectron	$[M+Na]^+$	1–7	nr	DP					0		B-type procyanidins (acetylated form)	Nonier et al. [36]
Grape seeds	Reflectron	$[M+Na]^+$	3–10	889.4–2910	DP					0		B-type procyanidins, galloylated	Vivas et al. [41]
			3–10	1041.5–3065.1	DP					1			
			3–9	1193.7–2927.2	DP					2			
			3–9	1346.0–3080.8	DP					3			
			5–8	2074.8–2943.0	DP					4			
Grape seeds	Reflectron	$[M+Na]^+$	1–5	nr	DP					0		B-type procyanidins, galloylated	Weber et al. [50]
			1–5	nr	DP					1			
			2–5	nr	DP					2			
	Linear	$[M+Na]^+$	2–12	nr	DP					0			
			2–11	nr	DP					1			
			2–11	nr	DP					2			
			3–10, 12	nr	DP					3			
			4–10	nr	DP					4			
			5–8	nr	DP					5			

Table 2 (*Continued*)

Substrate	Mode[a]	Mass specie	DP range	Observed mass	CAT	FIS	AFZ	GCAT	ROB	Galloyl	A-type bond	Proanthocyanidin type	Reference
Grape seeds	Reflectron	$[M+Na]^+$	2–5	nr	DP					1		B-type procyanidins, galloylated	Mané et al. [45]
			4–6	nr	DP					2			
		$[M+K]^+$	2–7	nr	DP					0			
			2–7	nr	DP					1			
			4–6	nr	DP					2			
Grape berries		$[M+Na]^+$	2–11	601–3195	DP					0		B-type procyanidins, galloylated	Perret et al. [51]
			2–10	753–3059	DP					1			
Grape skins	Reflectron	$[M+Na]^+$	3–5	889.6–1465.9	DP			0		0		B-type procyanidins and prodelphidins, galloylated	Vivas et al. [41]
			3–4	1042.3–1330.8	DP			0		1			
			3–5	905–1482	DP-1			1		0			
Grape stems	Reflectron	$[M+Na]^+$	3–6	889.3–1754.1	DP			0		0		B-type procyanidins and prodelphidins, galloylated	Vivas et al. [41]
			3–4	1041.5–1329.4	DP			0		1			
			4–6	1193.4–1770.4	DP-1			1		0			
			4–6	1209.3–1785.5	DP-2			2		0			
			5	1514	2			3		0			
Sea buckthorn (*Hippophae rhamnoides*) pomace	Linear	$[M+Na]^+$	4–6	1180.2–1758.2	DP			0				B-type procyanidins and prodelphinidins	Rösch et al. [34]
			3–8	906.6–2351.9	DP-1			1					
			3–8	923.0–2364.8	DP-2			2					
			3–9	939.6–2672.1	DP-3			3					
			4–9	1244.7–2686.1	DP-4			4					
			5–10	1549.3–2990.1	DP-5			5					
			6–10	1853.6–3004.8	DP-6			6					
			7–11	2157.6–3308.5	DP-7			7					
			8–12	2462.3–3610.1	DP-8			8					
			9–12	2766.4–3631.0	DP-9			9					
			10–12	3069.6–3648.1	DP-10			10					
			11–13	3369.3–3947.3	DP-11			11					
			12	3962.2	0			12					
Hops (*Humulus Lupulus* L.)	Linear	$[M+Na]^+$	3–9	888.6–2618.7	DP			0				B-type procyanidins and prodelphinidins	Taylor et al. [17]
			3–10	904.2–2922.2	DP-1			1					
			3–9	920.1–2651.7	DP-2			2					
			5–8	1513.5–2378.6	DP-3			3					
			4	2395.5	0			4					
Cranberries		$[M+Na]^+$	4–7	1173–2038	DP						1	A-type procyanidins	Foo et al. [16]
Cranberries	Reflectron	$[M+Na]^+$	3–7	887–2039	DP			0			1	A- and B-type procyanidins and prodelphinidins	Porter et al. [52]
			3–6	903–1767	DP-1			1			1		
			5–8	1461–2326	DP			0			2		
			5–7	1477–2054	DP-1			1			2		
			6–9	1748–2612	DP			0			3		
			6–8	1764–2340	DP-1			1			3		
Cranberries	Reflectron	$[M+Cs]^+$	4–9	1285.2–2725.6	DP			0			1	A- and B-type procyanidins and prodelphinidins	Neto et al. [43]
			5–6, 8–9	1589.3–2741.7	DP-1			1			1		
			4–12	1283.3–3587.9	DP			0			2		
			4–10	1299.8–3027.7	DP-1			1			2		
			4–11	1281.3–3297.7	DP			0			3		
			5–11	1585.3–3313.8	DP-1			1			3		
			7, 9–10	2143.5–3007.7	DP			0			4		
			9–10	2735.7–3023.7	DP-1			1			4		
Sorghum (*Sorghum bicolor* (L.) *Moench*)	Reflectron	$[M+Cs]^+$	4–9	1287–2727	DP			0			0	A- and B-type procyanidins and prodelphinidins	Krueger et al. [42]
			4–6	1285–1861	DP			0			1		

			4–6	1283–1859	DP	0		2		
			4–6	1281–1857	DP	0		3		
			5–6	1567–1855	DP	0		4		
			6	1853	DP	0		5		
			4–9	1303–2743	DP-1	1		0		
			4–6	1301–1877	DP-1	1		1		
			4–6	1299–1875	DP-1	1		2		
			4–6	1297–1873	DP-1	1		3		
			4–9	1319–2759	DP-2	2		0		
			4–6	1317–1893	DP-2	2		1		
			4–6	1315–1891	DP-2	2		2		
			4–6	1313–1889	DP-2	2		3		
			5–6	1599–1887	DP-2	2		4		
Almond (*Prunus dulcis (Mill.) D.A. Webb*) skins	Linear	$[M+Na]^+$	1–6	313.1–1754.0	DP			0	A- and B-type properlagonidin, procyanidins and prodelphinidins	Monagas et al. [53]
			2–7	599.2–2039.6	DP			1		
			2–6	585.2–1737.4	DP-1	1		0		
			2, 4, 7	583.2, 1159.3, 2024.8	DP-1	1		1		
			2–5	617.2–1481.2	DP-1		1	0		
			2–6	615.2–1767.4	DP-1		1	1		

CAT: (epi)catechin; FIS: (epi)fisetinidol; AFZ: (epi)afzlechin; GCAT: (epi)gallocatechin; ROB: (epi)robinetinidol.
nr: not reported.
[a] Detector mode: reflectron or linear; polarity: positive.

of B-type and A-type linkages between units. Therefore, according to this equation it is implied that MALDI-TOF enables the interpretation of mass signals corresponding to differences in molecular weight attributed to the: (a) degree of hydroxylation in the A- or B-ring of the flavan-3-ol unit; (b) presence of galloylation; (c) nature of the interflavan linkage, and (d) DP. However, it does not allow to distinguish the different stereoisomers [44].

Both the reflectron and linear modes have been successfully applied to the analysis of proanthocyanidins. To illustrate the potential and limitations of both modes in the MALDI-TOF analysis, Fig. 2 depicts the spectra of peanut skin proanthocyanidins acquired from the application of the two modes (unpublished results). An equispaced series of signal groups corresponding to the polymeric distribution of the peanut proanthocyanidins is observed. In both spectra, the maximum intensity is obtained for the oligomers of DP4 ($[M+Na]^+ = 1173–1191$), and the relative peak intensities are equivalent up to DP6 ($[M+Na]^+ = 1749–1767$). However, for higher m/z, lower intensities or even no peaks are detected in the reflectron spectrum (Fig. 2b) in comparison to the linear spectrum (Fig. 2a). This lack of sensitivity for higher m/z is mainly due to the extra-focusing suffered by the ions into the reflectron. Oligomers higher than DP8 ($[M+Na]^+ = 2325$) could be detected working in the linear mode, but a fractionation of the extract would be necessary in order to increase their proportion in the sample. So, the linear mode provides better information about the mass distribution of the species present in the sample. However, if identification is pursued, the reflectron mode is the best choice. Its high mass resolution power allows to distinguish the mass of the isotopic peaks with enough accuracy to compare with the theoretical calculated mass. Fig. 3d shows how the resolution of monoisotopic peaks allows mass assignation. Nevertheless, in the linear mode the unresolved isotopic envelop for the oligomers of peanut proanthocyanidins higher than DP6 (Fig. 3b) is obtained, not allowing complete assessment of structural features. However, for the lower m/z range, mass resolution is enough to separate isotopic peaks in the spectra recorded by both modes (Fig. 3a and c).

The different types of proanthocyanidins reported in the literature for plant and non-plant foods are discussed below in increasing order of structural complexity.

3.2.1. Food plants

Apple proanthocyanidins are homopolymers constituted by (epi)catechin units linked by B-type linkages (or B-type procyanidins) (Table 2). Application of MALDI-TOF MS in the linear mode allowed the detection of apple procyanidins up to DP15 as $[M+Ag]^+$ [32]. Also using the same mode, Shoji et al. [33] reported a maximum DP of 10 both as $[M+Na]^+$ and $[M+K]^+$. Recently, $[M+Na]^+$ up to DP15 and $[M+K]^+$ up to DP13 have been reported for apple procyanidin fractions using the reflectron mode [45]. The pulp of coffee (DP6 as $[M+Na]^+$ in the linear mode) [46] and the Japanese quince fruit (*Chaenomeles japonica*) (DP9 as $[M+Na]^+$ and DP6 as $[M+K]^+$ in the reflectron mode) [47] are other plant foods exclusively constituted by (epi)catechins (Table 2). Finally, procyanidin homopolymers up to DP30 as $[M+K]^+$ have also been detected in the seed coat of brown soybean by MALDI-TOF using both the linear and reflectron modes [48].

Procyanidins could also be esterified with gallic acid as occurs in the case of pear and grape seed tannins (Table 2). Procyanidins up to DP24 in monogalloylated form have been reported in pear juice using a combination of linear and reflectron modes [49]. In the case of grape seeds, the comparison of the reflectron and linear positive modes has been the subject of several studies (Table 2). Mass data for grape seed proanthocyanidins has been reported as $[M+Na]^+$ although both $[M+Na]^+$ and $[M+K]^+$ have reported in one study [45]. Yang and Chien [38] reported procyanidins up to DP7 (galloyl ester units: up to 2) with the reflectron mode, whereas a maximum

Table 3
Structural characterization of proanthocyanidins from non-food plants by MALDI-TOF MS analysis.

Substrate	Mode[a]	Mass specie	DP range	Observed mass	CAT	FIS	AFZ	GCAT	ROB	Galloyl	A-type bond	Proanthocyanidin type	Reference
Willow leaves (*Salix alba*)	Linear	$[M+Na]^+$	3–8	nr	DP							B-type procyanidins	Behrens et al. [54]
Lime leaves (*Tilia cordata*)	Linear	$[M+Na]^+$	3–10	nr	DP							B-type procyanidins	Behrens et al. [54]
Spruce needles (*Picea abies*)	Linear	$[M+Na]^+$	3–10	nr	DP			0				B-type procyanidins and prodelphinidins	Behrens et al. [54]
			3	905	2			1					
			3	921	1			2					
Beach leaves (*Fagus sylvatica*)	Linear	$[M+Na]^+$	3–8	nr	DP		1					B-type properlagonidins, procyanidins and prodelphinidins	Behrens et al. [54]
			3	873	1			0					
			3	905	2			1					
			3	921	1			2					
			3	937	0			3					
Dock (*Rumex obtusifolius*)	Reflectron	$[M+Na]^+$	3–8	889–2331	DP					0	0	A- and B-type procyanidins, galloylated	Spencer et al. [40]
			3–6	887–1753	DP					0	1		
			3–7	1041–2195	DP					1	0		
			3–6	1039–1905	DP					1	1		
			3	1037	DP					1	2		
			2–10	905–2346	DP					2	0		
			3–4	1191–1479	DP					2	1		
			3–6	1345–2211	DP					3	0		
			4–6	1786–2362	DP					4	0		
			5–6	2226–2514	DP					5	0		
			6	2665	DP					6	0		
Flowers of *Trifolium* spp.	Reflectron	$[M+Na]^+$	3–7	889.1–2043.0	DP			0				B-type procyanidins and prodelphinidins	Meagher et al. [55]
			3–6	902.3–1770.0	DP-1			1					
			3–4	923.9–1209.1	DP-2			2					
			3–5	937.2–1513.0	DP-3			3					
			4–6	1241.1–1817.0	DP-4			4					
			5	1544.9	0			5					
			6–7	1848.8–2137.1	DP-6			6					
			7	2153.9	0			7					
Lotus corniculatus (var. Fargus)	Linear and reflectron	$[M+Na]^+$	4–6	1177–1754	DP			0				B-type procyanidins and prodelphinidins	Hedqvist et al. [56]
			4–6	1193–1769	DP-1			1					
			4–6	1209–1785	DP-2			2					
			4–6	1225–1801	DP-3			3					
			6	1817	DP-4			4					
Lotus spp.	Reflectron	$[M+Na]^+$	3–6	nr	DP			0			0	A- and B-type procyanidins and prodelphinidins	Sivakumaran et al. [39]
			3–6	nr	DP			0			1		
			3–6	nr	DP-1			1			0		
			3–6	nr	DP-1			1			1		
			3–6	nr	DP-2			2			0		
			3–6	nr	DP-2			2			1		
			3–6	nr	DP-3			3			0		
			3–6	nr	DP-3			3			1		
			4–6	nr	DP-4			4			0		
			4–6	nr	DP-4			4			1		
			5–6	nr	DP-5			5			0		
			5–6	nr	DP-5			5			1		
			6	nr	0			6			0		
			6	nr	0			6			1		
Bark of *Pinus pinaster*	Reflectron	$[M+Na]^+$	1–7	nr	DP					0		B-type procyanidins, galloylated	Weber et al. [50]
			1	nr	DP					1			
			2–5	nr	DP					2			

	Linear	$[M+Na]^+$	3–8	nr	DP			0			
			2–7	nr	DP			2			
Bark of *Pinus massoniana*	Reflectron	$[M+Na]^+$	1–7	nr	DP			0		B-type procyanidins, galloylated	Weber et al. [50]
			2–4	nr	DP			2			
	Linear	$[M+Na]^+$	2–13	nr	DP			0			
			2–12	nr	DP			2			
			4, 5, 7, 9, 10	nr	DP			4			
Bark of *Pinus radiata*	Reflectron	$[M+Na]^+$	2–8	1020.3–4009.4	DP		0			B-type procyanidins and prodelphinidins (acetylated form)	Ku and Mun [37]
			2–8	1078.3–4067.3	DP-1		1				
			2–7	1136.3–3627.5	DP-2		2				
			4–7	2190.1–3685.4	DP-3		3				
Heartwood of Quebracho (*Schinopsis balansae*)	Reflectron	$[M+Na]^+$	3–5	841.4–1385.6		DP		0		Profisetinidins and prorobinetinidins	Vivas et al. [41]
			3–7	857.4–1945.6		DP-1		1			
			3–8	873.4–2236.7		DP-2		2			
			6–7	1707.5–1979.6		DP-3		3			
			3–6	nr		DP		0			
Quebracho (*Schinopsis balansae)* tannin extract	Linear	$[M+Na]^+$	2–7	nr		DP-1		1		Profisetinidins and prorobinetinidins	Pasch et al. [57]
			2–10	nr		DP-2		2			
			5–7, 10	nr		DP-3		3			
Bark of *Acacia auriculiformis*	Linear	$[M+Na]^+$	3	858.7	2		0	1		Profisetinidins, prorobinetinidins and prodelphinidins	Ishida et al. [31]
			3	874.3	1		0	2			
			3	890.4	0		0	3			
			3	906.4	0		1	2			
			3	922.1	0		2	1			
			4	1128.3	3		0	1			
			4	1146.5	2		0	2			
			4	1162.6	1		0	3			
			4	1178.5	0		0	4			
			4	1194.5	0		1	3			
			4	1210.6	0		2	2			
			4	1226.2	0		3	1			
			5	1418.7	3		0	2			
			5	1434.5	2		0	3			
			5	1450.5	1		0	4			
			5	1466.5	0		0	5			
			5	1482.4	0		1	4			
			5	1498.6	0		2	3			
			5	1514.0	0		3	2			
Mimosa bark (*Acacia mearnsii)* tannin extract	Linear	$[M+Na]^+$	2	nr	0		0	2		Profisetinidins, prorobinetinidins and prodelphinidins	Pasch et al. [57]
			3	nr	2		0	1			
			3	nr	1		0	2			
			3	nr	0		0	3			
			3	nr	0		1	2			
			3	nr	0		2	1			
			4	nr	2		0	2			
			4	nr	1		0	3			
			4	nr	0		0	4			
			4	nr	0		1	3			
			4	nr	0		2	2			

CAT: (epi)catechin; FIS: (epi)fisetinidol; AFZ: (epi)afzelechin; GCAT: (epi)gallocatechin; ROB: (epi)robinetinidol.
nr: not reported.

[a] Detector mode: reflectron or linear; polarity: positive.

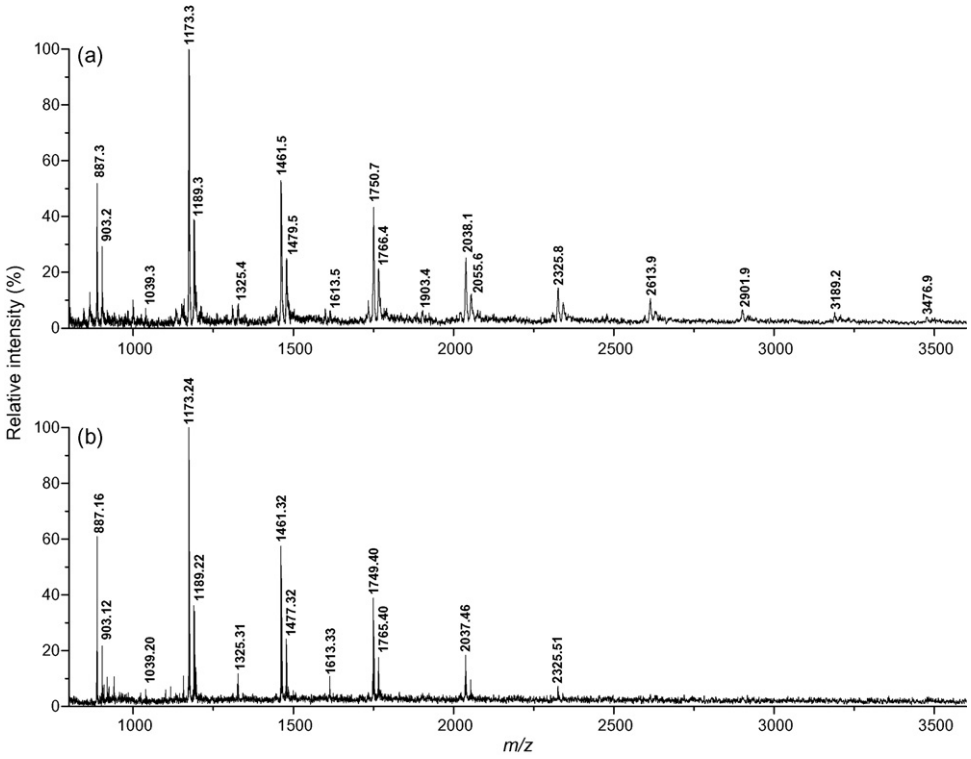

Fig. 2. MALDI-TOF spectra of peanut skin extracts in linear (a) and reflectron (b) modes.

DP of 9 (galloyl ester units: up to 5) was obtained with the linear mode (Table 2). These findings were consistent with parallel work performed by Krueger et al. [35], but a slightly higher DP and degree galloylation were found in this case: maximum DP of 9 and 11 (galloyl ester units: up to 4 and 6) for the reflectron and linear modes, respectively. More recently, Weber et al. [50] reported a maximum DP of 12 (galloyl ester units: 5) with the linear mode, although the results reported for the reflectron mode were more scarce (maxi-

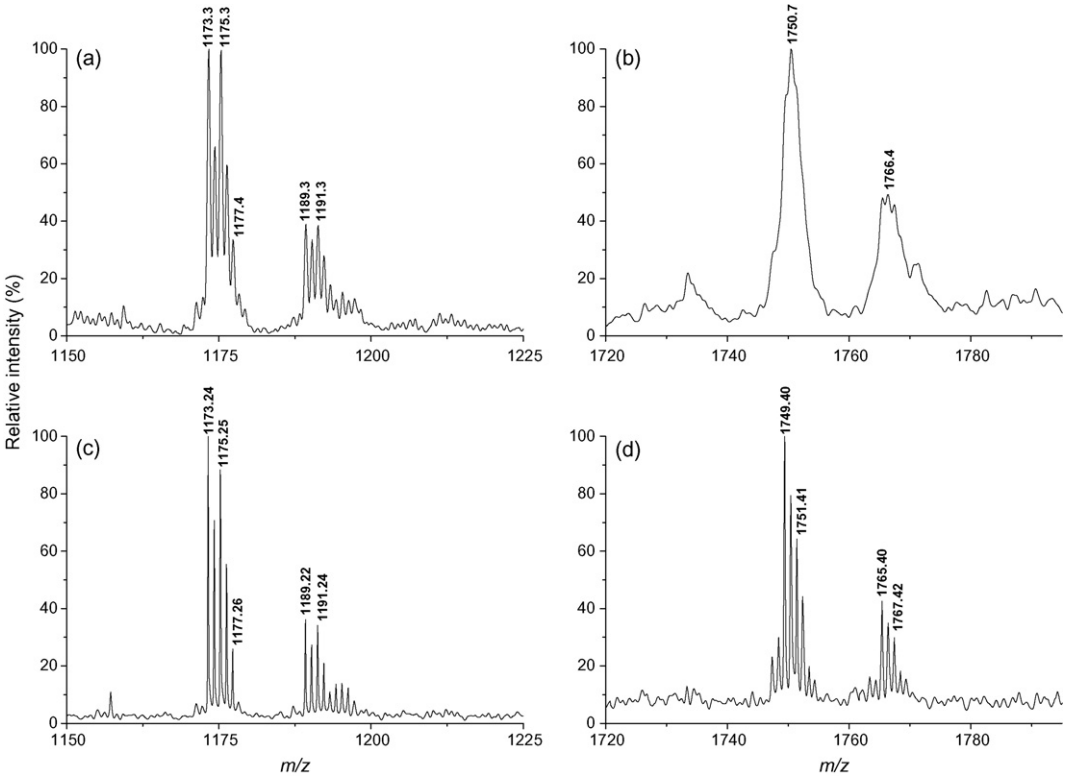

Fig. 3. $[M+Na]^+$ ion signal of A-type procyanidin and prodelphinidin tetramers (a, c) and hexamers (b, d) obtained on a MALDI-TOF spectrometer in linear (top) and reflectron (bottom) modes.

mum DP: 5; galloyl ester units: up to 2). The reflectron mode has been the choice of the remaining studies found in the literature [36,41,45] (Table 2). Among these studies, Vivas et al. [41] reported procyanidins up to DP10 (galloyl ester units: up to 4) with this mode. Although some MALDI-TOF mass signals have been interpreted as belonging to proanthocyanidins containing (epi)gallocatechin units [38] or as A-type polymers [35], it is generally accepted that grape proanthocyanidins are exclusively constituted by partially galloylated (epi)catechin units linked by B-type interflavonoid linkages. Finally, another aspect which is important to highlight from the characterization of grape seed proanthocyanidins by MALDI-TOF analysis is the fact that the degree of galloylation seems to decrease with increasing DP (Table 2).

In contrast to grape seeds, grape skins and stems also contain (epi)gallocatechins units and therefore are constituted by both B-type procyanidins and prodelphinidins (Table 2). They are found as heteroproanthocyanidins with low level of galloylation. MALDI-TOF analysis of grape skins has revealed the presence of proanthocyanidins constituted up to DP5 containing a maximum number of 1 (epi)gallocatechin unit and 1 galloyl ester unit [41]. In the case of grape stems, proanthocyanidins up to DP6, containing 1 (epi)gallocatechin and up to 2 galloyl ester units have been found [41]. Whole grape berries have been also analyzed by MALDI-TOF MS but only monogalloylated procyanidins up to DP10 have been reported [51]. Sea buckthorn pomace (*Hippophaë rhamnoides*) and hops (*Humulus Lupulus* L.) are another plant foods constituted by B-type procyanidins and prodelphinidins (Table 2). $[M+Na]^+$ of prodelphinidins homopolymers up to DP12, and procyanidin–prodelphinidin heteropolymers up to DP13 have been detected in sea buckthorn pomace by MALDI-TOF MS in the linear mode [34]. In the case of hops, pure procyanidins up to DP9 or combined with 1–4 (epi)gallocatechin units up to DP10, have been detected as $[M+Na]^+$ in the linear mode [17]. A special structural feature of sea buckthorn pomace proanthocyanidins was the increase of (epi)gallocatechin units with increasing DP, whereas the contrary was observed for hop proanthocyanidins (Table 2).

Proanthocyanidins in plant food such as cranberries and sorghum occur as A- and B-type procyanidins and prodelphinidins (Table 2). The presence of A-type proanthocyanidins in cranberries was first reported by Foo et al. [16], who detected procyanidins up DP7 as $[M+Na]^+$ containing up to 1 A-type linkage. Porter et al. [52] later confirmed that cranberries were composed by both procyanidin and prodelphinidin units in the form of heteropolymers up to DP9 as $[M+Na]^+$ containing only 1 (epi)gallocatechin unit and up to 3 A-type linkages. Subsequent studies using cesium trifluoroacetate as cationizing agent, enable the detection in the reflectron mode of a procyanidin–prodelphinidin heteropolymer series up DP9 containing up to 4 A-type linkages and no more than 1 (epi)gallocatechin unit, once again confirming the abundance of A-type linkages and the predominance of epi(catechin) units in cranberries [43]. Sorghum proanthocyanidins present a higher degree of structural complexity. MALDI-TOF analysis in the reflectron mode has demonstrated the presence of proanthocyanidins up to DP9 as $[M+Cs]^+$ composed of pure (epi)catechin units containing up to 5 A-type linkages, or as heteropolymers constituted by 1–4 (epi)gallocatechins with up to 4 A-type linkages [42]. Heterogeneity was even higher in the case of almond skin proanthocyanidins (Table 2). Using MALDI-TOF MS in the linear mode, proanthocyanidins up to DP7 composed of (epi)catechins combined with 1 (epi)afzelechin unit or 1 (epi)gallocatechin unit linked by B-linkages and by no more than 1 A-type linkage were detected [53].

3.2.2. Non-food plants

The potential of MALDI-TOF technique in the characterization of proanthocyanidins can also be demonstrated by its application to non-plant food species (Table 3). Proanthocyanidins from foliages such as willow leaves (*Salix alba*), beach leaves (*Fagus sylvatica*) and lime leaves (*Tilia cordata*), as well as needles from spruce (*Picea abies*), which play an important role in carbon and nitrogen cycling in soils, have been analyzed by MALDI-TOF MS using the linear mode [54]. $[M+Na]^+$ corresponding to B-type procyanidins up to DP8 and DP10 have been detected in willow and lime leaves, respectively. Proanthocyanidins from spruce needles are constituted by (epi)catechins up to DP10 but may also contain (epi)gallocatechin units [54]. More complex beach leaves proanthocyanidins occurred as pure procyanidin polymers up to DP8 or as mixtures containing (epi)afzelechin or (epi)gallocatechin units [54].

Dock (*Rumex obtusifolius*), *Trifolium* spp. and *Lotus* spp. are important forage cultivars and proanthocyanidin sources for ruminants (Table 3). Recent application of MALDI-TOF MS in the reflectron mode revealed the presence of procyanidins in dock up to DP8 as $[M+Na]^+$ containing up to 6 A-type linkages and a maximum of 2 galloylated units [40]. Proanthocyanidins in the flowers of *Trifolium* spp. and in *Lotus* spp. were presented as both procyanidin and prodelphinidin homopolymers and as a complex series of procyanidin–prodelphinidin heteropolymers. Using MALDI-TOF in the reflectron mode, heteropolymers up to DP7 as $[M+Na]^+$ containing up to 6 (epi)gallocatechin units were detected in the flowers of *Trifolium* spp. [55]. Proanthocyanidins in *Lotus* spp. additionally presented A-type linkages and consisted of heteropolymers up to DP6 as $[M+Na]^+$ with increasing number of (epi)gallocatechins up to 6 units and containing no more than 1 A-type linkage [39]. However, in particular, the Fargus variety (*Lotus corniculatus*) only presented B-type procyanidins and prodelphinidins [56].

Wood proanthocyanidins are presented in diverse structural forms, from simple homopolymers to complex heteropolymers, constituted by both phloroglucinol and resorcinol A-type ring flavanol-3-ol units (Table 3). By the application of the reflectron mode, proanthocyanidins exclusively composed of (epi)catechin units up to DP7 and containing up to 2 galloylated units were detected in the bark of *Pinus pinaster* and *P. massonlana* as $[M+Na]^+$, whereas the linear mode revealed the existence of polymers up to DP8 (galloyl ester units: up to 2) and DP13 (galloyl ester units: up to 4) for *P. pinaster* and *P. massonlana*, respectively [50]. In *P. radiata* (epi)catechin homopolymers up to DP8 or combined with up to 3 (epi)gallocatechin units were detected as $[M+Na]^+$ in the reflectron mode [37]. Using MALDI-TOF MS also in the reflectron mode, profisetinidins up to DP8 and DP10 were detected as $[M+Na]^+$ in the heartwood of Quebracho (*Schinopsis balansae*) [41] and in an industrial Quebracho tannin extract [57] respectively, containing up to 3 (epi)robinetidin units in both cases. Heterogeneity was higher in the bark of *Acacia auricalformis* [31] and *A. mearnsii* [57] which additionally contained (epi)gallocatechins resulting in complex profisetinidin–prorobinetinidin–prodelphinidin heteropolymers up to DP5 and DP8, respectively.

3.3. Assessment of the molecular weight distribution of proanthocyanidins by MALDI-TOF MS

MALDI-TOF sensitivity decreases with increasing molecular weight of proanthocyanidins, as have been demonstrated for hop [17] and apple proanthocyanidins [45]. This limits the use of the absolute intensity of mass signals provided by MALDI-TOF to obtain of a full molecular weight distribution analysis of highly polydisperse polymers. However, after fractionation, good correlation between the mean DP obtained from MALDI-TOF and ^{13}C spectroscopy was obtained for a cranberry oligomeric fraction presenting a narrow molecular weight distribution (mean DP = 4.7) [16]. On the other hand, fractionation of a hop proanthocyanidin extract to separate small oligomers that reach the detector first (leading to saturation), significantly improved the sensitivity of

the detection of large molecular weight proanthocyanidins under MALDI-TOF analysis in comparison to a total extract [17]. However, it did not completely overcome the discrimination of high molecular weight polymers. Factors associated with the behaviour of high molecular weight polymers themselves including suppression of ionization, reduction of desorption and in-source fragmentation leading to formation of non-covalent ion clusters, have been reported to influence the detection of high molecular masses by MALDI-TOF MS [17,58].

In order to minimize some problems associate with the behaviour of the high molecular weight proanthocyanidins under MALDI-TOF MS, Mané et al. [45] recently proposed a method based on the protein complexation of proanthocyanidins using bovine serum albumin (BSA). By this binding action, the BSA protects the polymer against fragmentation and the same time serve as charge carrier limiting differences in ionization efficiency among the different proanthocyanidin structure [45,58]. BSA–tannin complexes were detected as an unresolved hump under MALDI-TOF. By subtracting the intensity of the BSA signal from that of BSA–tannin complex for each m/z value, the molecular weight distribution of proanthocyanidin could be estimated by the calculation of the number-average molecular weight ($M_n = \Sigma(m/z)_i I_i / \Sigma I_i$, where I_i is the absolute intensity), weight-average molecular weight ($M_w = \Sigma(m/z)_i^2 I_i / \Sigma(m/z)_i I_i$) and the polidispersity index (PI). Results found from the application of this approach to polymeric proanthocyanidin fractions from apples were in good agreement with those obtained by thiolysis [45].

3.4. Conclusions

In conclusion, results from the application of MALDI-TOF MS to the analysis of plant proanthocyanidins summarized in the present review, clearly demostrate that it is a powerful tool for the structural elucidation of these complex polymers. Sample preparation protocols including: sample concentration, matrix and cationizing agent selection and concentration, and sample-to-matrix ratio, have been successfully standardized in last decade. Advantages and limitation of the use of the reflectron or linear modes for identification purposes have also been clearly established. However, quantification by MALDI-TOF MS is still a great challenge due to the discrimination of high molecular weight polymers. The chemical behaviour of highly polymerized proanthocyanidins under MALDI-TOF MS seems to be an important aspect that limits the use of this technique for quantitative analysis. Improvements in mass detection have been achieved by fractionating the proanthocyanidin extract, separating low from high molecular weight species. In this way, the measurement could be quantitative at least in a low mass range. More effort should be made on the acquisition of uniform response over whole mass range of proanthocyanidin distribution.

Acknowledgements

This work has received financial support from projects AGL2007-66772/ALI, AGL2007-28594-E/ALI and ANALYSIC S-505/AGR-0312. M.M is recipient of a “Ramón y Cajal” postdoctoral contract (RYC-2008-03190).

References

[1] P.M. Aron, J.A. Kennedy, Mol. Nutr. Food Res. 52 (2008) 79–104.
[2] L.J. Porter, in: J.B. Harbone (Ed.), The Flavonoids, Chapman and Hall, New York, 1988, pp. 21–62.
[3] W. Hümmer, P. Schreier, Mol. Nutr. Food Res. 52 (2008) 1381–1398.
[4] J.A. Kennedy, G.P. Jones, J. Agric. Food Chem. 49 (2001) 1740–1746.
[5] L. Gu, M.A. Kelm, J.F. Hammerstone, G. Beecher, J. Holden, D. Haytowitz, R.L. Prior, J. Agric. Food Chem. 51 (2003) 7513–7521.
[6] J.F. Hammerstone, S.A. Lazarus, A.E. Mitchell, R. Rucker, H.H. Schmitz, J. Agric. Food Chem. 47 (1999) 490–496.
[7] S.A. Lazarus, G.E. Adamson, J.F. Hammerstone, H.H. Schmitz, J. Agric. Food Chem. 47 (1999) 3693–3701.
[8] J.B. Fenn, M. Mann, C.K. Meng, S.F. Wong, C.M. Whitehouse, Science 246 (1989) 64–71.
[9] M. Karas, F. Hillenkamp, Anal. Chem. 60 (1988) 2299–2301.
[10] K. Tanaka, H. Wadi, Y. Ido, S. Akita, Y. Yoshida, T. Yoshida, Rapid Commun. Mass Spectrom. 2 (1988) 151–153.
[11] M. Karas, U. Bahr, Trends Anal. Chem. 9 (1990) 321–325.
[12] D.C. Schriemer, L. Li, Anal. Chem. 68 (1996) 2721–2725.
[13] V. Cheynier, H. Fulcrand, P. Sarni, M. Moutounet, Analusis 25 (1997) M14–M21.
[14] S. Guyot, T. Doco, J.M. Souquet, M. Moutounet, J.F. Drilleau, Phytochemistry 44 (1997) 351–357.
[15] H. Fulcrand, S. Remy, J.M. Souquet, V. Cheynier, M. Moutounet, J. Agric. Food Chem. 47 (1999) 1023–1028.
[16] L.Y. Foo, Y. Lu, A.B. Howell, N. Vorsa, Phytochemistry 54 (2000) 173–181.
[17] A.W. Taylor, E. Barofsky, J.A. Kennedy, M.L. Deinzer, J. Agric. Food Chem. 51 (2003) 4101–4110.
[18] C.G. Herbert, R.A.W. Johnstone, Mass Spectrometry Basics, CRC Press LLC, Boca Raton, Florida, 2003.
[19] H. Ehring, M. Karas, F. Hillenkamp, Org. Mass Spectrom. 27 (1992) 472–480.
[20] M. Karas, M. Glückmann, J. Schafer, J. Mass Spectrom. 35 (2000) 1–12.
[21] W.C. Chang, L.C. Huang, Y.-S. Wang, W.-P. Peng, H.C. Chang, N.Y. Hsu, W.B. Yang, C.H. Chen, Anal. Chim. Acta 582 (2007) 1–9.
[22] C. Dass, Fundamentals of contemporary mass spectrometry, John Wiley & Sons, Hoboken, New Jersey, 2007.
[23] Y. Xu, M.L. Bruening, J.T. Watson, Mass Spectrom. Rev. 22 (2003) 429–440.
[24] J.H. Gross, Mass Spectrometry: A Textbook, Springer-Verlag, Heidelberg, 2004.
[25] B.H. Wang, K. Dreisewerd, U. Bahr, M. Karas, F. Hillenkamp, J. Am. Soc. Mass Spectrom. 4 (1993) 393–398.
[26] R.S. Brown, J.J. Lennon, Anal. Chem. 67 (1995) 1998–2003.
[27] M.W. Duncan, H. Roder, S.W. Hunsucker, Brief Funct. Genom. Proteom. 7 (2008) 355–370.
[28] H. Chen, M. He, J. Am. Soc. Mass Spectrom. 16 (2005) 100–106.
[29] D.C. Grant, R.J. Helleur, Anal. Bioanal. Chem. 391 (2008) 2811–2818.
[30] E. Szajli, T. Feher, K.F. Medzihradszky, Mol. Cell. Proteom. 7 (2008) 2410–2418.
[31] Y. Ishida, K. Kitagawa, K. Goto, H. Ohtani, Rapid Commun. Mass Spectrom. 19 (2005) 706–710.
[32] M. Ohnishi-Kameyama, A. Yanagida, T. Kanda, T. Nagata, Rapid Commun. Mass Spectrom. 11 (1997) 31–36.
[33] T. Shoji, S. Masumoto, N. Moriichi, T. Kanda, Y. Ohtake, J. Chromatogr. A 1102 (2006) 206–213.
[34] D. Rösch, C. Mugge, V. Fogliano, L.W. Kroh, J. Agric. Food Chem. 52 (2004) 6712–6718.
[35] C.G. Krueger, N.C. Dopke, P.M. Treichel, J. Folts, J.D. Reed, J. Agric. Food Chem. 48 (2000) 1663–1667.
[36] M.F. Nonier, C. Absalon, N. Vivas, N. Vivas De Gaulejac, J. Chromatogr. A 1033 (2004) 291–297.
[37] C.S. Ku, S.P. Mun, Wood Sci. Technol. 41 (2007) 235–247.
[38] Y. Yang, M. Chien, J. Agric. Food Chem. 48 (2000) 3990–3996.
[39] S. Sivakumaran, W. Rumball, G.A. Lane, K. Fraser, L.Y. Foo, M. Yu, L.P. Meagher, J. Chem. Ecol. 32 (2006) 1797–1816.
[40] P. Spencer, S. Sivakumaran, K. Fraser, L.Y. Foo, G.A. Lane, P.J.B. Edwards, L.P. Meagher, Phytochem. Anal. 18 (2007) 193–203.
[41] N. Vivas, M.F. Nonier, N. Vivas De Gaulejac, C. Absalon, A. Bertrand, M. Mirabel, Anal. Chim. Acta 513 (2004) 247–256.
[42] C.G. Krueger, M.M. Vestling, J.D. Reed, J. Agric. Food Chem. 51 (2003) 538–543.
[43] C.C. Neto, C.G. Krueger, T.L. Lamoureaux, M. Kondo, A.J. Vaisberg, R.A.R. Hurta, S. Curtis, M.D. Matchett, H. Yeung, M.I. Sweeney, J.D. Reed, J. Sci. Food Agric. 86 (2006) 18–25.
[44] J.D. Reed, C.G. Krueger, M.M. Vestling, Phytochemistry 66 (2005) 2248–2263.
[45] C. Mané, N. Sommerer, T. Yalcin, V. Cheynier, R.B. Cole, H. Fulcrand, Anal. Chem. 79 (2007) 2239–2248.
[46] M.A. Ramirez-Coronel, N. Marnet, V.S.K. Kolli, S. Roussos, S. Guyot, C. Augur, J. Agric. Food Chem. 52 (2004) 1344–1349.
[47] M. Strek, S. Gorlach, A. Podsedek, D. Sosnowska, M. Koziolkiewicz, Z. Hrabec, E. Hrabec, J. Agric. Food Chem. 55 (2007) 6447–6452.
[48] Y. Takahata, M. Ohnishi-Kameyama, S. Furuta, M. Takahashi, I. Suda, J. Agric. Food Chem. 49 (2001) 5843–5847.
[49] N.E. Es-Safi, S. Guyot, P.H. Ducrot, J. Agric. Food Chem. 54 (2006) 6969–6977.
[50] H.A. Weber, A.E. Hodges, J.R. Guthrie, B.M. O'Brien, D. Robaugh, A.P. Clark, R.K. Harris, J.W. Algaier, C.S. Smith, J. Agric. Food Chem. 55 (2007) 148–156.
[51] C. Perret, R. Pezet, R. Tabacchi, Phytochem. Anal. 14 (2003) 202–208.
[52] M.L. Porter, C.G. Krueger, D.A. Wiebe, D.G. Cunningham, J.D. Reed, J. Sci. Food Agric. 81 (2001) 1306–1313.
[53] M. Monagas, I. Garrido, R. Lebrón-Aguilar, B. Bartolomé, C. Gómez-Cordovés, J. Agric. Food Chem. 55 (2007) 8498–8507.
[54] A. Behrens, N. Maie, H. Knicker, I. Kogel-Knabner, Phytochemistry 62 (2003) 1159–1170.
[55] L.P. Meagher, K. Widdup, S. Sivakumaran, R. Lucas, W. Rumball, J. Agric. Food Chem. 54 (2006) 5482–5488.
[56] H. Hedqvist, I. Mueller-Harvey, J.D. Reed, C.G. Krueger, M. Murphy, Anim. Feed Sci. Technol. 87 (2000) 41–56.
[57] H. Pasch, A. Pizzi, K. Rode, Polymer 42 (2001) 7531–7539.
[58] H. Fulcrand, C. Mané, S. Preys, G. Mazerolles, C. Bouchut, J.P. Mazauric, J.M. Souquet, E. Meudec, Y. Li, R.B. Cole, V. Cheynier, Phytochemistry 69 (2008) 3131–3138.